Molecular Genetics and Metabolism 119 (2016) 57–67

Contents lists available at ScienceDirect

Molecular Genetics and Metabolism

journal homepage: www.elsevier.com/locate/ymgme

Ammonium accumulation is a primary effect of 2-methylcitrate exposure in an *in vitro* model for brain damage in methylmalonic aciduria

Hong-Phuc Cudré-Cung [a], Petra Zavadakova [a], Sónia do Vale-Pereira [a], Noémie Remacle [a], Hugues Henry [b], Julijana Ivanisevic [c], Denise Tavel [d], Olivier Braissant [e], Diana Ballhausen [a,*]

[a] Center of Molecular Diseases, Lausanne University Hospital, Switzerland
[b] Biomedicine, Innovation & Development, Lausanne University Hospital, Switzerland
[c] Metabolomics Research Platform, Faculty of Biology and Medicine, University of Lausanne, Switzerland
[d] Department of Physiology, Lausanne University, Switzerland
[e] Biomedicine, Lausanne University Hospital, Switzerland

ARTICLE INFO

Article history:
Received 29 June 2016
Received in revised form 27 July 2016
Accepted 27 July 2016
Available online 30 July 2016

Keywords:
2-Methyl citric acid or 2-methylcitrate
Methylmalonic aciduria
Brain development
Neurotoxicity
Ammonium
Apoptosis

ABSTRACT

Using 3D organotypic rat brain cell cultures in aggregates we recently identified 2-methylcitrate (2-MCA) as the main toxic metabolite for developing brain cells in methylmalonic aciduria. Exposure to 2-MCA triggered morphological changes and apoptosis of brain cells. This was accompanied by increased ammonium and decreased glutamine levels. However, the sequence and causal relationship between these phenomena remained unclear. To understand the sequence and time course of pathogenic events, we exposed 3D rat brain cell aggregates to different concentrations of 2-MCA (0.1, 0.33 and 1.0 mM) from day *in vitro* (DIV) 11 to 14. Aggregates were harvested at different time points from DIV 12 to 19. We compared the effects of a single dose of 1 mM 2-MCA administered on DIV 11 to the effects of repeated doses of 1 mM 2-MCA. Pan-caspase inhibitors Z-VAD FMK or Q-VD-OPh were used to block apoptosis.

Ammonium accumulation in the culture medium started within few hours after the first 2-MCA exposure. Morphological changes of the developing brain cells were already visible after 17 h. The highest rate of cleaved caspase-3 was observed after 72 h. A dose-response relationship was observed for all effects. Surprisingly, a single dose of 1 mM 2-MCA was sufficient to induce all of the biochemical and morphological changes in this model. 2-MCA-induced ammonium accumulation and morphological changes were not prevented by concomitant treatment of the cultures with pan-caspase inhibitors Z-VAD FMK or Q-VD-OPh: ammonium increased rapidly after a single 1 mM 2-MCA administration even after apoptosis blockade.

We conclude that following exposure to 2-MCA, ammonium production in brain cell cultures is an early phenomenon, preceding cell degeneration and apoptosis, and may actually be the cause of the other changes observed. The fact that a single dose of 1 mM 2-MCA is sufficient to induce deleterious effects over several days highlights the potential damaging effects of even short-lasting metabolic decompensations in children affected by methylmalonic aciduria.

1. Introduction

Methylmalonic aciduria (MMAuria) is an inborn error of metabolism characterized by the deficiency of the enzyme methylmalonyl-CoA mutase (EC 5.4.99.2). This enzyme is involved in the catabolic pathways of branched-chain amino acids, pyrimidines, odd-chain fatty acids and cholesterol side-chains [1–3]. This enzymatic dysfunction provokes the accumulation of putative toxic compounds proximal to the enzymatic block in body tissues and fluids, mainly methylmalonic acid (MMA), propionic acid and 2-methylcitrate (2-MCA) [4].

Neurologic complications are a major concern in MMAuria, as they can be severe and result in a permanent handicap [5,6]. Movement disorders, seizures and mental retardation are the main neurologic symptoms [7]. The characteristic bilateral lesion of basal ganglia usually occurs during episodes of metabolic decompensation [1]. The pathological mechanisms responsible for the neurologic deterioration in MMAuria are still poorly understood.

Abbreviations: 2-MCA, 2-methylcitrate; CNS, central nervous system; DIV, day *in vitro*; DMSO, dimethyl sulfoxyde; GalC, galactocerebroside; GDH, glutamate dehydrogenase; GFAP, glial fibrillary acidic protein; GS, glutamine synthetase; HRP, horseradish peroxidase; LC3, microtubule-associated protein 1A/1B-light chain 3; MBP, myelin basic protein; MMA, methylmalonic acid; MMAuria, methylmalonic aciduria; MRPL12, mitochondrial ribosomal protein L12; NH_4^+, ammonium; PBS, phosphate-buffered saline; p-NFM, medium weight phosphorylated neurofilament.

* Corresponding author.
E-mail address: diana.ballhausen@chuv.ch (D. Ballhausen).

http://dx.doi.org/10.1016/j.ymgme.2016.07.013

The current understanding of the mechanisms leading to neurodegeneration in MMAuria relies on two hypotheses: the "toxic metabolite hypothesis" suggests that metabolites accumulating in MMAuria are toxic for the central nervous system (CNS) [8,9]. The second hypothesis, "the trapping hypothesis", proposes that these putatively toxic metabolites are trapped and accumulate in the brain because of a limited flux out of the CNS through the blood-brain barrier [10]. Moreover, it is also thought that the metabolites are autonomously produced in the brain due to the presence of the metabolic defect in neurons [11]. As a consequence, these metabolites reach very high concentrations in the CNS leading to brain damage [8].

Based on these two hypotheses, the toxic role of the metabolites accumulating in MMAuria was investigated. Studies have mainly focused on the neurotoxicity of MMA, until it was suggested that MMA might be neurotoxic synergistically with propionyl-CoA and 2-MCA [12]. Altogether, these studies suggest that impairment of mitochondrial energy metabolism, secondary excitotoxicity and oxidative stress contribute to the pathogenesis of MMAuria [13–20].

3D organotypic brain cell aggregates derived from rat embryos are highly organized cultures resembling the *in vivo* developing brain structure and functions. They display great advantages for the study of inborn errors of metabolism affecting the CNS as they contain all types of brain cells and allow the study of different stages of brain development [21–23]. We previously developed an *in vitro* model of MMAuria in brain cell aggregates, by exposing these cultures to the different metabolites accumulating in this disease [24]. Our previous work in 3D aggregates indicated 2-MCA as the most toxic metabolite. Besides MMAuria, 2-MCA is known to accumulate in propionic aciduria and to a lesser extent in cobalamine and biotin deficiencies. Administration of 2-MCA altered the morphology of astrocytes, oligodendrocytes and neurons and increased cell death by apoptosis. Furthermore, ammonium (NH_4^+) levels in culture medium increased while glutamine levels decreased after administration of 2-MCA [24]. These findings were present at day *in vitro* (DIV) 14. However, the starting time of these events and their chronological order were unknown.

Based on our recent results, this study examined the time course of previously observed effects induced by 2-MCA in 3D brain cell aggregates and followed these aggregates over a longer period of time than in our previous study. We also administered the pan-caspase inhibitors Z-VAD FMK and Q-VD-OPh in some cultures to prevent apoptosis in order to identify the events related to caspase activation. Moreover, we investigated the effects of a single dose of 1 mM 2-MCA compared to repeated applications of 1 mM 2-MCA.

2. Material and methods

2.1. Ethics statement

This study was carried out in strict accordance with the Ethical Principles and Guidelines for Scientific Experiments on Animals of the Swiss Academy for Medical Sciences. The protocol was approved by the Ethics Committee for Animal Experimentation. The rats had sufficient amount of food and water during the transportation period and before their sacrifice.

2.2. 3D organotypic rat brain cell cultures in aggregates

Pregnant Sprague–Dawley rats (Charles-River, France) were sacrificed by decapitation on day 15 of gestation. The decapitation was followed by removal of embryos. Fetal whole brains were extracted, pooled and mechanically dissociated. 3.6×10^7 cells were grown in 8 ml of a serum-free, chemically-defined medium with 25 mM glucose and maintained under constant gyratory agitation at 37 °C, in an atmosphere of 10% CO_2 and 90% humidified air to form reaggregated 3D primary brain cell cultures as previously described [25,26]. Media were replenished every three days from DIV 5 until DIV 14, and every two days from DIV 14 on, by exchanging 5 ml of medium per culture. When culture media were removed they were kept at −80 °C until biochemical analysis. On the day of harvest, aggregate pellets were washed three times with ice-cold phosphate-buffered saline (PBS) and either embedded for histology in embedding compound (Tissue-Tek O.C.T. Compound, Sakura Finetek, Netherlands) and frozen in liquid nitrogen-cooled 2-methylbutane (Sigma-Aldrich, Germany), or directly frozen in liquid nitrogen and kept at −80 °C until analysis.

2.3. Treatment protocols

The metabolite 2-MCA (Ernesto Brunet-Romero, Madrid, Spain) was buffered in PBS and the pH was adjusted to 7.5. Cultures were grown according to three different protocols (Fig. 1A–C). In protocol A, cultures were treated with 0.1, 0.33 or 1 mM 2-MCA 6 times every 12 h from DIV 11 to DIV 14; aggregates were harvested 5 h after the treatment on DIV 12, 13, 14, 15, 17 and 19. In protocol B, cultures were treated with a single dose of 1 mM 2-MCA on DIV 11; aggregates were harvested on DIV 14 and 15. In protocol C, the pan-caspase inhibitors Z-VAD FMK (Enzo Life Sciences, USA) or Q-VD-OPh (Sigma-Aldrich, Germany) were added to 2-MCA-treated cultures and controls.

Z-VAD FMK was solubilized in dimethyl sulfoxyde (DMSO, Sigma-Aldrich, Germany) and further diluted in culture medium, leading to a final concentration of 0.2% DMSO in culture flask. Z-VAD FMK was added at a final concentration of 100 μM per culture flask on DIV 11 in controls and 1 mM 2-MCA-treated cultures (Fig. 1C1). Q-VD-OPh was solubilized in DMSO and further diluted in culture medium, leading to a final concentration of 0.05% DMSO in culture flask. Q-VD-OPh was added at a final concentration of 10 μM per culture flask on DIV 11 in controls and 1 mM 2-MCA-treated cultures (Fig. 1C2). DMSO alone was also treated as control condition to verify its potential toxicity for the aggregates. Aggregates and culture medium were harvested on DIV 14 as previously described.

2.4. Immunofluorescence

Immunofluorescence was carried out on 16 μm aggregate cryosections using antibodies against different markers of brain cell types. All antibodies used in this study were commercially available and raised against the following antigens: GalC (mouse monoclonal anti-galactocerebroside, 1:100, Millipore, MAB342); GFAP (mouse monoclonal anti-glial fibrillary acidic protein, 1:100, Millipore, MAB360); p-NFM (mouse monoclonal anti-medium weight phosphorylated neurofilament 160 kDa, clone NN18, 1:200, Millipore, MAB5254); MBP (mouse monoclonal anti-myelin basic protein, 1:100, Santa Cruz Biotechnology, Inc., sc-66064). Secondary antibodies were goat anti-mouse IgG labeled with Alexa Fluor® 555 (red), chicken anti-mouse IgG labeled with Alexa Fluor® 488 (green) or donkey anti-goat IgG labeled with Alexa Fluor® 488 (green). Sections were fixed for 1 h in 4% paraformaldehyde (Sigma-Aldrich, Germany) in PBS at room temperature and washed in PBS (3 × 5 min). Non-specific antibody binding sites were blocked with 1% bovine serum albumin in PBS (BSA-PBS; Sigma-Aldrich, Germany) for 1 h. Primary antibodies diluted in 1% BSA-PBS were applied to sections and further detected with the corresponding secondary antibodies.

Labeling of microglia with Isolectin IB_4 Alexa Fluor® 568 dye conjugate (I21412, Invitrogen, USA) was proceeded as above-mentioned, but the secondary antibody was omitted.

Detection of cleaved caspase-3 (rabbit polyclonal anti-cleaved Caspase-3, Asp175, 1:1000, Cell Signaling, 9661) in aggregates was performed with the Tyramide Signal Amplification Kit (Life Technologies, USA). Aggregate cryosections (16 μm) were subjected to the same procedure as described above. In addition, endogenous peroxidase activity was quenched with 1.5% H_2O_2 in PBS (Sigma-Aldrich, Germany) followed by washes with PBS (3 × 5 min). Non-specific antibody binding sites were blocked for 1 h at room temperature with the blocking buffer of

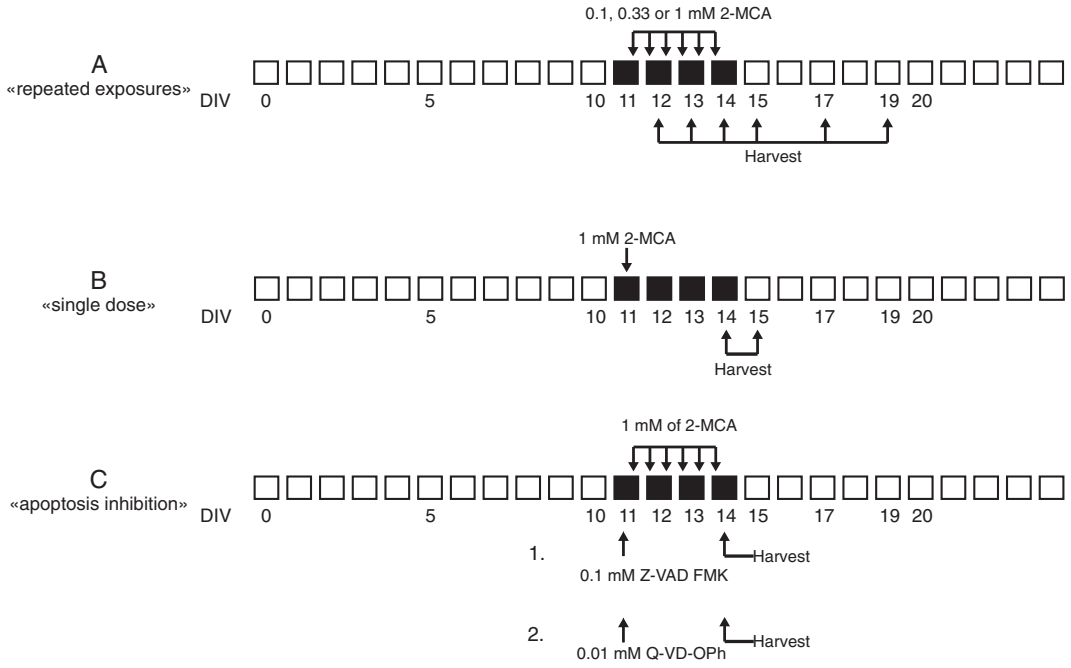

Fig. 1. Treatment protocols. Brain cell aggregates were treated and harvested according to three different protocols: (A) Different concentrations of 2-MCA (0.1/0.33/1 mM) were administered six times, from DIV 11 to 14, every 12 h. Aggregates were harvested on DIV 12, 13, 14, 15, 17 and 19. (B) A single dose of 1 mM 2-MCA was administered on DIV 11. Aggregates were harvested on DIV 14 and 15. (C) 1 mM 2-MCA was administered six times, from DIV 11 to 14, every 12 h. Additionally, 0.1 mM Z-VAD FMK (C1) or 0.01 mM Q-VD-OPh (C2) was administered on DIV 11 to inhibit apoptosis. Aggregates were harvest on DIV 14.

the kit. The primary antibody against the large fragment (17/19 kDa) of cleaved caspase-3 (Cell Signaling Technology, USA) diluted 1:1000 in blocking buffer was applied to sections overnight at 4 °C. After washing, sections were incubated with a horseradish peroxidase (HRP) conjugated anti-rabbit IgG secondary antibody (provided by the kit) for 1 h. Peroxidase staining was performed using Alexa Fluor® 555-labeled tyramide diluted 1:200 in amplification buffer (provided by the kit) and applied to sections for 10 min. Negative controls were processed the same but omitting the primary antibody, resulting in no staining.

Sections were then mounted under FluorSave™ (Merck Millipore, Germany), observed and photographed using an Olympus BX50 microscope equipped with a UC30 digital camera (Olympus, Japan).

2.5. Western blot analyses

Aggregates were homogenized in 150 mM sodium chloride, 50 mM Tris–HCl, pH 8.0, 1% NP-40 (Sigma-Aldrich, Germany) and Protease Inhibitor Cocktail - Complete Mini (Roche Applied Science, Switzerland), and sonicated for 5 s. Lysates were cleared by centrifugation at 12,000 rpm for 30 min at 4 °C.

After dilution, the protein content was measured by bicinchoninic acid assay (Thermo Scientific, USA) and diluted to a final concentration of 1.2 μg/μl in NuPAGE® LDS Sample Buffer (Life Technologies, USA). Samples were heated at 70 °C for 10 min and resolved on NuPAGE® 4–12% Bis–Tris Gel using NuPAGE® MOPS SDS Running Buffer (Life Technologies, USA) at a constant voltage (200 V, 60 min). Proteins were transferred onto nitrocellulose membranes, 0.45 μm (Millipore, USA). Membranes were blocked with 5% non-fat dry milk in TBS-Tween (20 mM Trizma base, 137 mM NaCl, 0.05% Tween, pH 7.6) for 1 h at room temperature. After blocking, the membranes were incubated overnight with primary antibodies diluted in 3% non-fat dry milk and TBS-Tween. The membranes were probed with HRP-conjugated secondary antibodies and developed by chemiluminescence (ECL Western Blotting Detection Reagents; GE Healthcare, France). All antibodies used in this study were commercially available and raised against the following antigens: cleaved caspase-3 (rabbit polyclonal anti-cleaved caspase-3, Asp175, 1:1000, Cell Signaling, 9661), LC3 (rabbit polyclonal anti-microtubule-associated protein 1A/1B-light chain 3, 1:1000, Novus Biologicals, NB100-2220), α-fodrin (mouse monoclonal anti-α-fodrin, 1:3000, Enzo Life Sciences, AA6), glutamine synthetase (mouse monoclonal anti-glutamine synthetase, clone GS-6, 1:1000, Millipore, MAB302), NeuN (mouse monoclonal anti-NeuN clone A60, 1:750, Millipore, MAB377), NFM (mouse monoclonal anti-NFM clone NF-09, 1:1000, Santa Cruz, sc-51683), nonphosphorylated-NFM (mouse monoclonal anti-NFM, clone RMO44, 1:1000, Invitrogen, 13-0500), GFAP (mouse monoclonal anti-GFAP, 1:2500, Millipore, MAB360), actin (goat polyclonal anti-actin, clone I-19, 1:1000, Santa Cruz, sc1616), MRPL12 (rabbit polyclonal anti-mitochondrial ribosomal protein L12, 1:3000, Proteintech, 14795-1-AP). Secondary antibodies were HRP conjugated goat anti-mouse, anti-rabbit or rabbit anti-goat IgG (Vector Laboratories).

Images were taken with a Luminescent Image Analyzer LAS-4000 (Fujifilm; Life Science) and quantified with the public Java-based image processing program ImageJ (National Institutes of Health). Data acquired in arbitrary densitometric units were normalized to the reference protein and transformed to percentages of the densitometric levels obtained from scans of control samples visualized on the same blots.

2.6. Glutamine synthetase activity

Frozen aggregates were thawed in 0.4 ml of 2 mM potassium phosphate containing 1 mM EDTA (pH 6.8), homogenized by sonication, divided into aliquots and stored at −80 °C. Protein concentrations were determined by the method of Lowry [27] using bovine serum albumin as a standard. Glutamine synthetase (GS, EC 6.3.1.2) activity was assayed by a modification [28] of the method of Pishak and Phillips [29]. L-[1-^{14}C] glutamic acid was used as precursor, and phosphoenolpyruvate/pyruvate kinase as the ATP-regenerating system.

2.7. Basic metabolites and amino acids in culture media

200 μl of culture medium were taken for measurement of NH_4^+ and were replaced with fresh culture medium. NH_4^+ was measured on an Integra automatic analyzer (Roche, Switzerland); glucose and lactate were measured on a Cobas 8000 (Roche, Switzerland); free amino

acids were analyzed on an amino acid analyzer (Biochrom, UK); as described previously [24,30].

2.8. Intracellular glutamic acid and glutamine quantification

Glutamic acid and glutamine were measured by isotope-dilution high performance liquid chromatography coupled to high resolution mass spectrometry (LC-MS HR), as described below. A stock solution containing glutamic acid and glutamine at 0.35 mM in 0.1 N HCl was prepared. The resulting stock solution was further diluted in 60 mg/ml BSA in PBS to form the calibration solutions with final concentrations of 10, 20, 40, 60, 80 and 100 μM. An internal standard mix of 12 stable isotopes including d3-glutamic acid (Cambridge Isotope Laboratories, labeled amino acids set A) was used at a concentration of 1.25 mM in 0.1% (v/v) formic acid in water.

Calibration standards and samples (5 μl) were added to 45 μl of 0.1% (v/v) formic acid and mixed with 250 μl of acetonitrile containing the internal standards at a final concentration of 5 μM in a 96 × 1 ml deep well plate. After shaking for 10 min at 1200 rpm, the plate was incubated for 30 min at −20 °C and centrifuged at 4000*g* at 4 °C for 30 min. The supernatants (200 μl) were transferred to a new 96-well plate, sealed, and transferred to the LC-MS autosampler for analysis.

Chromatographic analysis was performed using an Accela pump (Thermo Scientific) and a PAL System autosampler (Thermo Scientific, CTC Analysis). Separation of the amino acids was achieved using an Acquity UPLC® BEH Amide column (1.7 μm 2.1 mm × 150 mm, Waters). The mobile phases consisted of H_2O with 20 mM ammonium formate and 0.1% (v/v) formic acid (mobile phase A), acetonitrile (mobile phase B). The flow rate was 400 μl/min throughout and the gradient increased linearly from 5% A, 95% B to 40% A, 60% B within 20 min.

Detection was performed using an orbitrap Q-Exactive mass spectrometer (Thermo Scientific). The instrument was equipped with an electrospray interface and was controlled by Xcalibur software version 2.2 (Thermo Scientific). The samples were analyzed in the positive-ionization mode in full scan mode with a scan range from 70 to 1000 *m/z*, at a resolution of 70,000.

Calibration curves were computed using the ratio of the peak area of the amino acids glutamic acid and glutamine and their internal standard d3-glutamic acid with a weighted (1/x) linear regression analysis.

2.9. Statistics

All data points are expressed as mean ± standard deviation (SD), unless specify otherwise. Statistical difference was determined with Student's *t*-test with $p < 0.05$.

3. Results

3.1. Rapid extracellular NH_4^+ accumulation

NH_4^+ levels were measured from 6 h after the first 2-MCA administration (DIV 11) to DIV 19 (Fig. 2). The onset and degree of NH_4^+ accumulation depended on the administered concentrations of 2-MCA. NH_4^+ already rose significantly 6 h after the first 1 mM 2-MCA treatment. For lower 2-MCA concentrations (0.1 and 0.33 mM) the NH_4^+ increase started slightly later, 12 h after the first treatment. The maximal mean NH_4^+ concentrations measured in culture media after repeated 2-MCA administration were 1748 μM on DIV 16 after exposure to 1 mM 2-MCA, 984.5 μM on DIV 14 with 0.33 mM 2-MCA, and 360.5 μM on DIV 12 with 0.1 mM 2-MCA. This represents up to 15 times of the NH_4^+

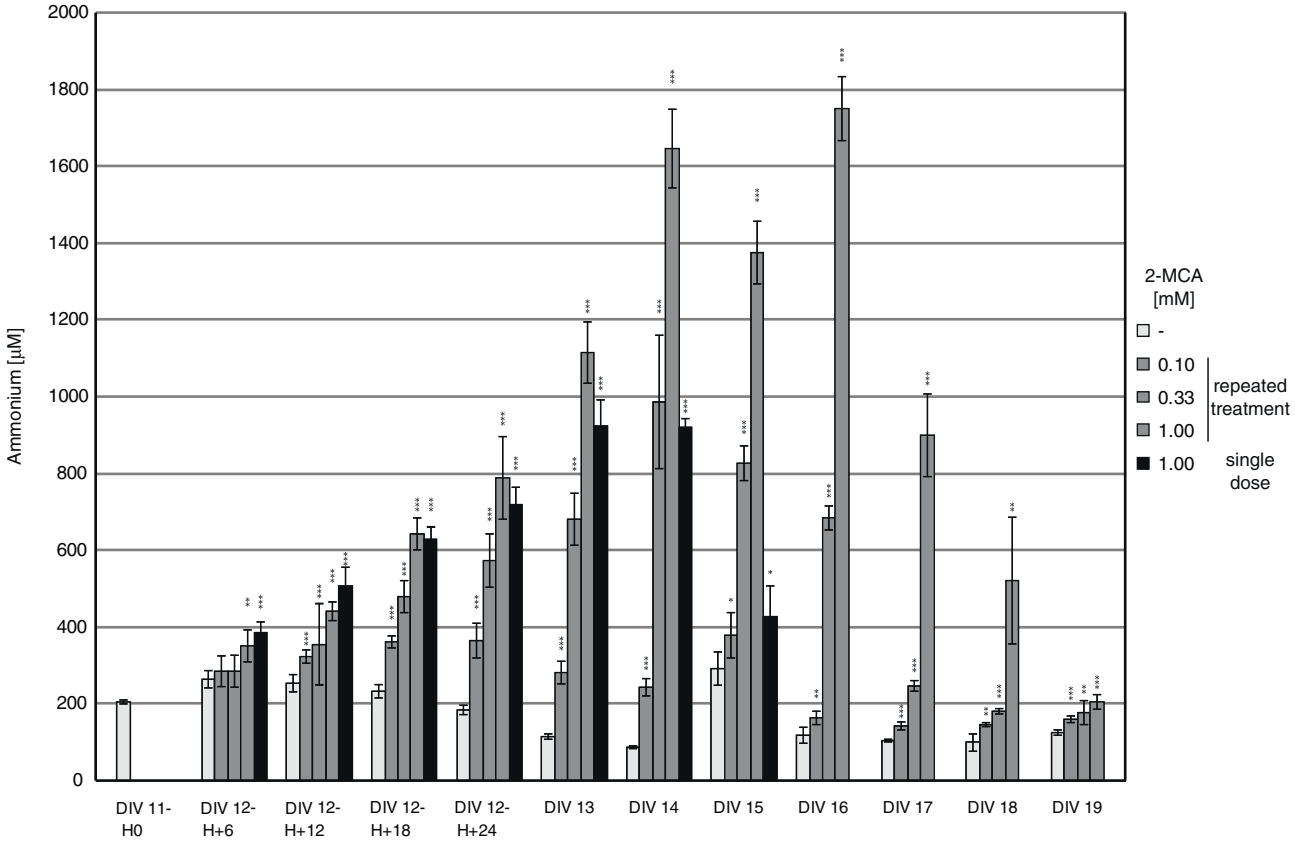

Fig. 2. Rapid extracellular NH_4^+ accumulation under 2-MCA exposure. NH_4^+ concentrations (μM) were measured in culture medium at different time points, from 6 h after the first treatment until DIV 19 in controls, cultures treated with repeated doses of 0.1/0.33/1 mM 2-MCA, or cultures treated with a single dose of 1 mM 2-MCA. Data shown as mean ± SD ($n = 3$ or 4); Student's *t*-test: $^*p < 0.05$, $^{**}p < 0.01$, $^{***}p < 0.001$.

concentration in control cultures for exposure to 1 mM 2-MCA. The maximal NH_4^+ concentration was reached earlier and started to drop down earlier for lower concentrations of 2-MCA. The NH_4^+ level observed on DIV 15 in cultures exposed to 1 mM 2-MCA is most probably due to a dilution effect caused by the change of 5/8 ml of culture medium on DIV 14, at a stage when aggregates continued to produce NH_4^+ under 2-MCA exposure. Five days after the end of 2-MCA administrations (DIV 19) NH_4^+ levels were still significantly higher for all concentrations compared to control cultures. A single dose of 1 mM 2-MCA administered on DIV 11 also induced significant NH_4^+ accumulation with a similar time course, but the maximal NH_4^+ mean concentration was reached on DIV 13 and stayed lower at 922 μM compared to repeated administration of 1 mM 2-MCA (Fig. 2).

3.2. Decreased extracellular glutamine levels, increased intracellular glutamine levels and glutamine synthetase activity

GS is the main enzyme responsible for NH_4^+ detoxification in the CNS through synthesis of glutamine in astrocytes. Therefore, we examined GS activity and expression in aggregates and glutamine levels in culture medium to see whether this pathway was affected by 2-MCA.

Glutamine levels in culture medium of treated aggregates were reduced compared to controls, starting from DIV 12 (Fig. 3A). The decrease of glutamine levels depended on the administered 2-MCA concentrations. The lowest glutamine concentrations were observed on DIV 14 for all concentrations. A single dose of 1 mM 2-MCA on DIV 11 also provoked a decrease of glutamine levels, which normalized on DIV 15, earlier compared to repeated administration of 1 mM 2-MCA. No other amino acid levels in culture medium were altered by 2-MCA administration (data not shown).

GS activity was measured in aggregates on DIV 14. A 40% decrease was observed after repeated administration of 1 mM 2-MCA (Fig. 3B). Lower 2-MCA concentrations and a single dose of 1 mM 2-MCA did not significantly alter GS activity (data not shown). GS protein expression was also quantified by western blot. No significant change was observed between control and treated cultures (data not shown).

Intracellular glutamine measurements showed about two-fold increase of glutamine content in 2-MCA treated aggregates (mean = 2122 μmol/L/g proteins, $n = 2$) compared to control aggregates (mean = 1121 μmol/L/g proteins, $n = 2$) while glutamate concentrations did not show any significant difference.

3.3. Metabolic profile

From DIV 11 to 13, no significant difference was observed between control and treated cultures regarding glucose and lactate levels in culture medium. On DIV 14, as previously described [24], a decrease of glucose was observed in cultures exposed repeatedly to 1 mM 2-MCA, while a significant increase of lactate was measured under repeated exposure to 0.33 as well as 1 mM 2-MCA (Fig. 4). No other change in glucose and lactate was found at lower 2-MCA concentrations as well as with a single dose of 1 mM 2-MCA.

3.4. Morphological changes of developing brain cells

Aggregates were stained with different antibodies to identify brain cell types and to examine how 2-MCA affected their morphology at different developmental stages.

The first effects of 2-MCA on developing brain cells were already visible after 17 h on DIV 12. As previously described [24], a dose response relationship was also observed in this study. Moreover, a single dose of 1 mM 2-MCA was already sufficient to induce all observed morphological alterations.

3.4.1. Astrocyte swelling

Astrocytes were already affected on DIV 12, 17 h after the first administration of the different 2-MCA concentrations. Swelling of astrocyte cell bodies and thickening of astrocyte fibers increased progressively over time until DIV 15. In aggregates exposed to 2-MCA, there were areas devoid of GFAP staining, suggesting the loss of astrocytes in these areas (Fig. 5). On DIV 19, swollen astrocytes and thick fibers had disappeared; GFAP was evenly localized along astrocytic fibers in controls and 2-MCA-treated aggregates at all 2-MCA concentrations as shown by immunohistochemistry. Semi-quantitative determination of GFAP by western blots did not reveal any significant change in GFAP expression, suggesting that the GFAP gene regulation was probably not affected by 2-MCA exposure. However, GFAP was a suitable marker to follow the astrocytic morphological changes in 2-MCA

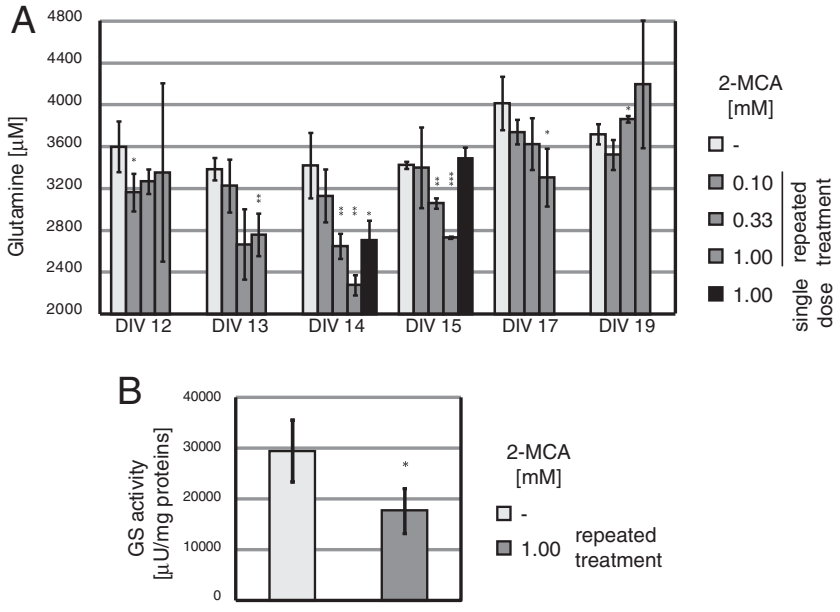

Fig. 3. Reduced extracellular glutamine and GS activity under 2-MCA exposure. (A) Glutamine levels [μM] were measured in culture medium from DIV 11 to DIV 19 in controls, cultures treated with repeated doses of 0.1/0.33/1 mM 2-MCA, or cultures treated with a single dose of 1 mM 2-MCA. Data shown as mean ± SD ($n = 3$); Student's t-test: $^*p < 0.05$, $^{**}p < 0.01$, $^{***}p < 0.001$. (B) GS activity [μU/mg proteins] was measured in controls and 1 mM 2-MCA-treated aggregates harvested on DIV 14. Data shown as mean ± SD ($n = 4$).

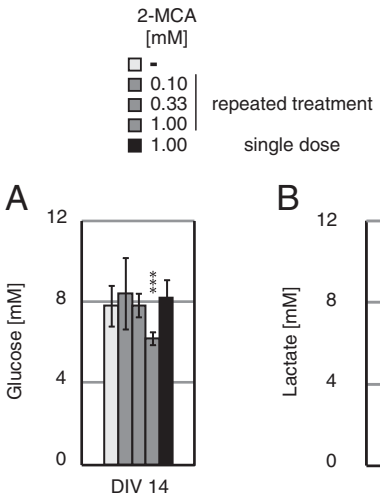

Fig. 4. Extracellular glucose and lactate levels on DIV 14. Glucose and lactate concentrations [mM] were measured in culture medium from DIV 12 to 19 in controls, cultures treated with repeated doses of 0.1/0.33/1 mM 2-MCA, or cultures treated with a single dose of 1 mM 2-MCA. Data shown as mean ± SD ($n = 3$ to 7); Student's t-test: $^{*}p < 0.05$, $^{**}p < 0.01$, $^{***}p < 0.001$.

exposed cultures over time. With a single dose of 1 mM 2-MCA, the same morphological alterations were observed on DIV 14 and 15.

3.4.2. Altered processing of neurofilaments

Labeling of p-NFM showed protein retention in neuronal bodies of aggregates exposed to 2-MCA compared to controls, starting on DIV 12. Reduced density of axonal fibers was observed at more advanced stages (Fig. 6). From DIV 15 to DIV 19, the difference between treated and control aggregates was less pronounced. Western blot with antibodies against total NFM, nonphosphorylated-NFM and NeuN did not reveal any significant change (data not shown). Similar effects were observed in aggregates exposed to a single dose of 1 mM 2-MCA.

3.4.3. Delayed maturation of oligodendrocytes

Two different antibodies were used to identify oligodendrocytes. When GalC, a marker for oligodendrocytes, was used, no change was observed between treated and control aggregates. However, when using MBP, a marker labeling myelin in more differentiated oligodendrocytes, a decrease of signal intensity was observed in all treated aggregates from DIV 13 and persisted on DIV 19 (Fig. 7). This might indicate a significant effect of 2-MCA on oligodendrocyte maturation. A single dose of 2-MCA was sufficient to induce a decrease of MBP signal intensity on DIV 14 and 15.

3.4.4. Microglia

Labeling of microglia with Isolectin IB_4 did not reveal significant changes between controls and cultures exposed to different 2-MCA concentrations (data not shown).

3.5. Highest apoptosis rate on DIV 14

Cleaved caspase-3 levels were examined in aggregates by immunohistochemistry (Fig. 8A) and western blot (Fig. 8B) from DIV 12 to DIV 19 to determine the time course of apoptosis under 2-MCA exposure. No difference was observed between control and 2-MCA treated aggregates on DIV 12 and 13. On DIV 14 the highest levels of cleaved caspase-3 were observed for all concentrations of 2-MCA and diminished progressively thereafter. As previously described [24], the increase of cleaved caspase-3 levels depended on the administered concentration of 2-MCA. But even a single dose of 1 mM 2-MCA was sufficient to induce an increase in cleaved caspase-3 at DIV 14.

Western blotting with an antibody against α-fodrin showed increased levels of the caspase-3 cleaved fragment of α-fodrin on DIV 14 in 2-MCA treated aggregates compared to controls (Fig. 8C), which is consistent with the findings above. In contrast, no change was observed

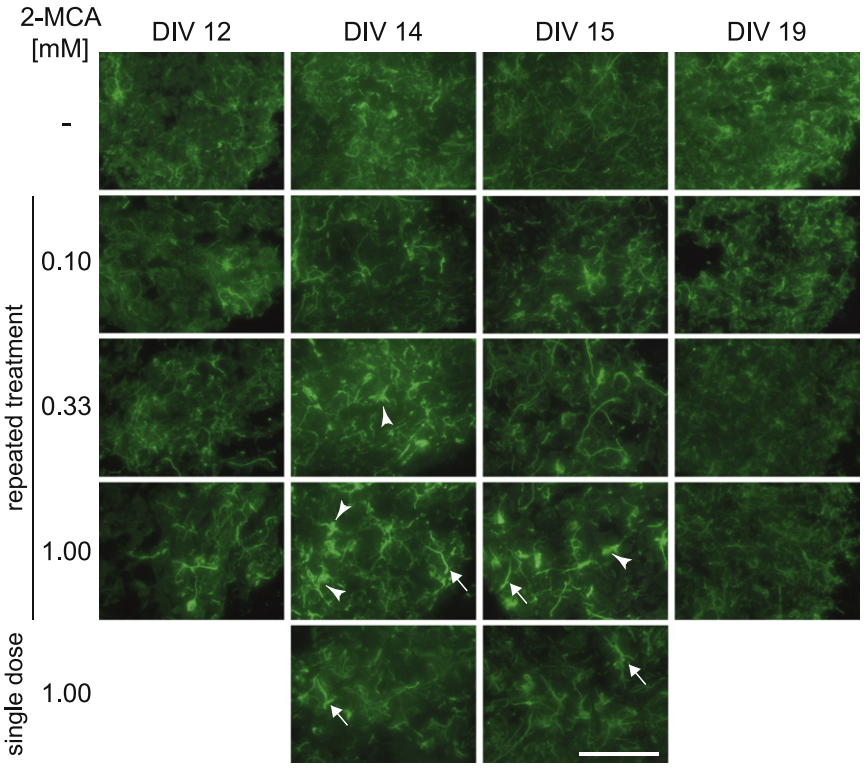

Fig. 5. Astrocyte swelling (arrow heads) and thickening of their primary fibers (arrows) under 2-MCA exposure. Immunofluorescence for GFAP on DIV 12, 14, 15, and 19 in astrocytes of controls, cultures treated with repeated doses of 0.1/0.33/1 mM 2-MCA, or cultures treated with a single dose of 1 mM 2-MCA. Scale bar: 100 μm.

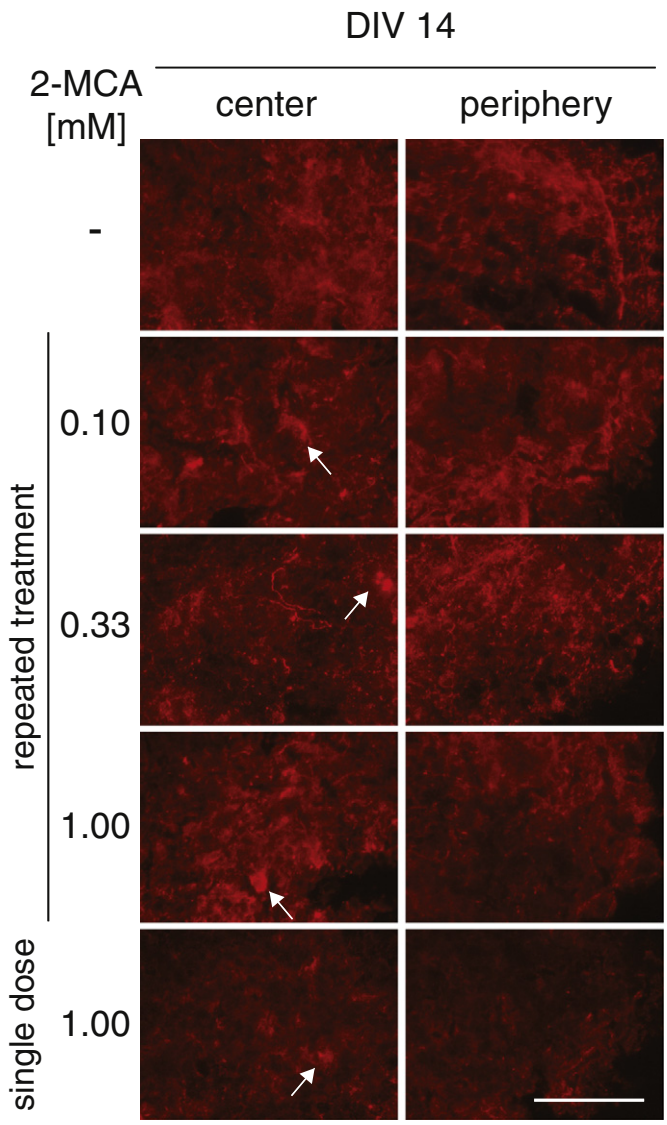

Fig. 6. p-NFM retention in neuronal cell bodies (arrows) and reduced density of axons under 2-MCA exposure. Immunofluorescence for p-NFM on DIV 14 in controls, cultures treated with repeated doses of 0.1/0.33/1 mM 2-MCA or cultures treated with a single dose of 1 mM 2-MCA. Left column: center of the aggregate cultures. Right column: periphery of the aggregate cultures. Scale bar: 100 μm.

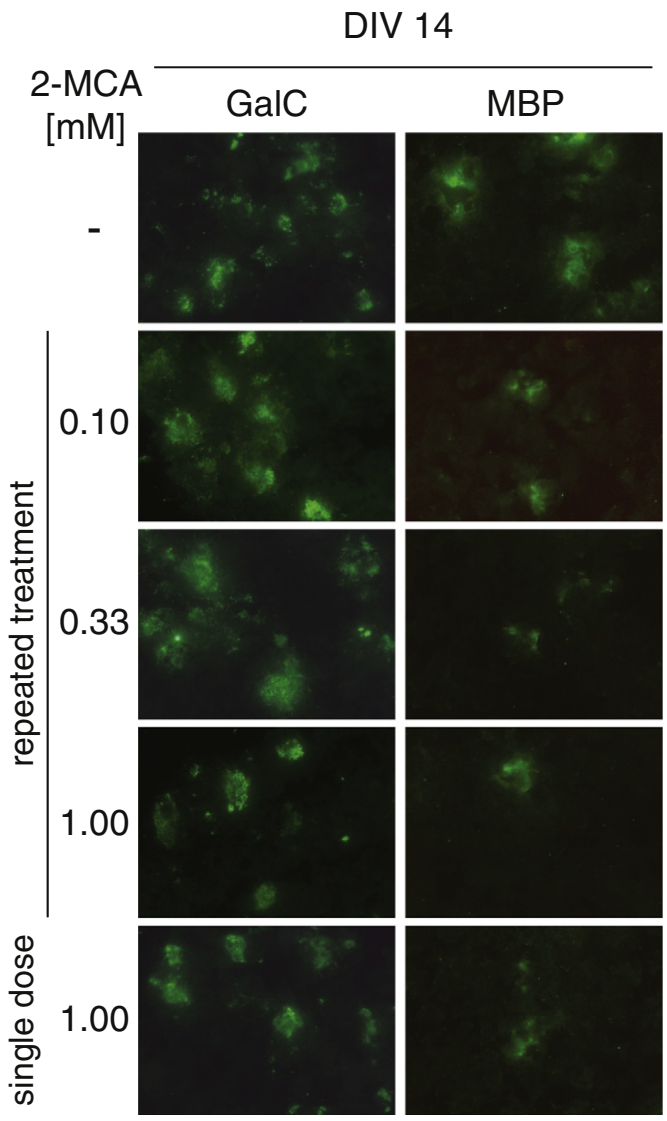

Fig. 7. Delayed myelination under 2-MCA exposure. Left column: Immunofluorescence for GalC on DIV 14 in oligodendrocytes of controls, cultures treated with repeated doses of 0.1/0.33/1 mM 2-MCA, or cultures treated with a single dose of 1 mM 2-MCA. No difference was observed between controls and treated cultures. Right column: Immunofluorescence for MBP on DIV 14 in oligodendrocytes of controls, cultures treated with repeated doses of 0.1/0.33/1 mM 2-MCA or cultures treated with a single dose of 1 mM 2-MCA. MBP expression was weaker in treated cultures as compared to controls. Scale bar: 100 μm.

with the calpain-cleaved fragment of α-fodrin, a marker of necrosis. Western blotting with an antibody against LC3, a marker for autophagy that may result in cell death, did not reveal significant differences between 2-MCA exposed aggregates and control aggregates (data not shown).

3.6. Pan-caspase inhibitors do not prevent biochemical and morphological changes

To analyze whether the 2-MCA-induced NH_4^+ accumulation preceded the increase of apoptosis, we inhibited apoptosis using the pan-caspase inhibitors Z-VAD FMK or Q-VD-OPh. Pan-caspase inhibitors were administered at the same time as the first 2-MCA exposure. Immunofluorescence and western blot with an antibody against cleaved caspase-3 showed that administration of these apoptosis inhibitors successfully inhibited caspase-3 activation (Fig. 9A, B), thereby preventing the occurrence of apoptosis. Despite successful apoptosis inhibition, NH_4^+ still accumulated in culture medium of treated aggregates (Fig. 9C). Glutamine decrease (Fig. 9D) and morphological alterations (Fig. 9E) also occurred despite apoptosis inhibition. These findings indicate that apoptosis *per se* was not the cause of either ammonium accumulation or the observed morphological and biochemical changes.

4. Discussion

The aim of the present study was to determine the time course of the effects recently observed after 2-MCA exposure in 3D rat brain cells aggregates under development [24]. We particularly wanted to determine the role of ammonium that was observed to accumulate in this *in vitro* model for brain damage in MMAuria.

4.1. Increased production of NH_4^+ precedes metabolic and morphological alterations

The earliest observed event was NH_4^+ accumulation in culture medium of aggregates treated with 2-MCA. It started within few hours after

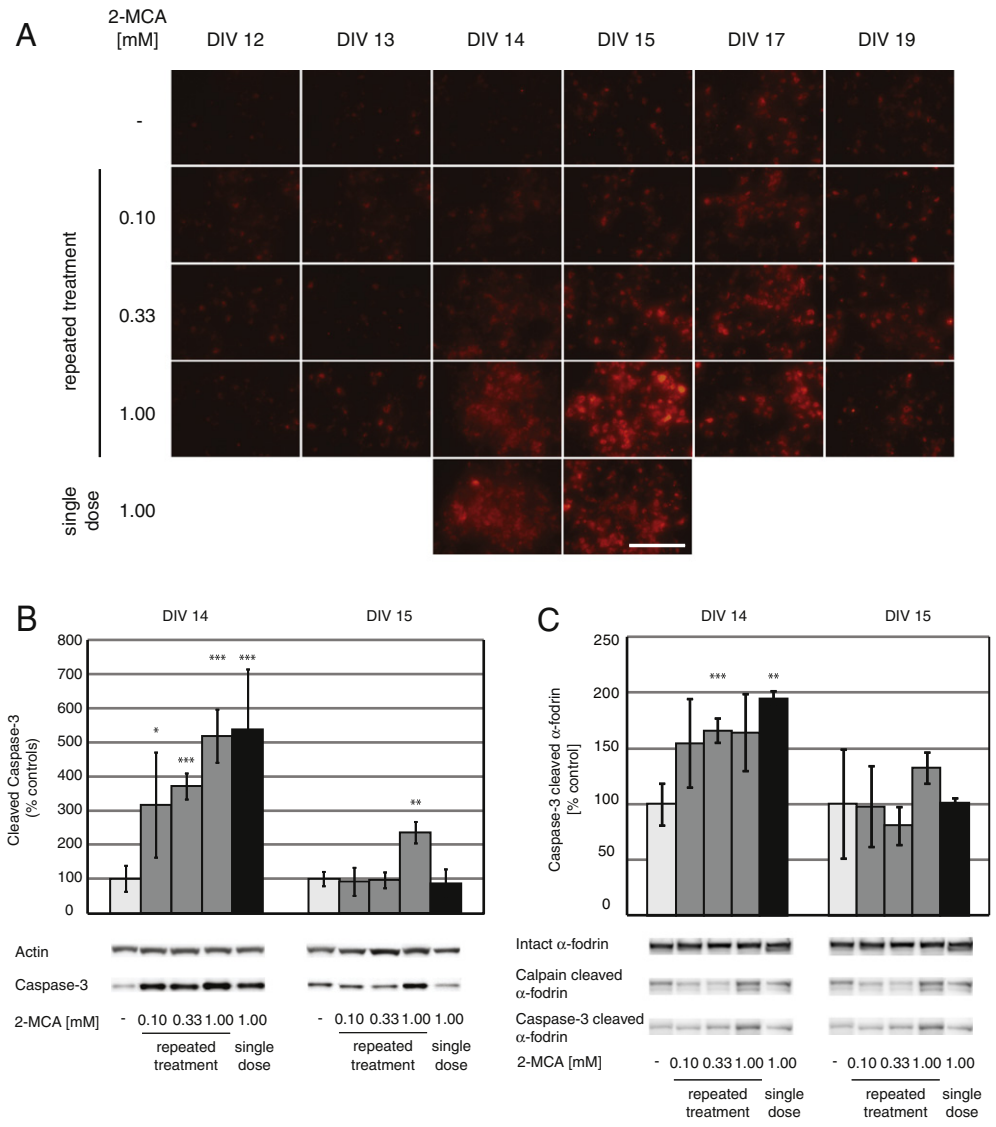

Fig. 8. Time course of apoptosis rate in brain cell aggregates exposed to 2-MCA. (A) Immunofluorescence for cleaved caspase-3 from DIV 12 to DIV 19 in control cultures, cultures treated with repeated doses of 0.1/0.33/1 mM 2-MCA, or cultures treated with a single dose of 1 mM 2-MCA. The strongest expression of cleaved caspase-3 was found on DIV 14 at all concentrations. Scale bar: 100 μm. (B) Western blot for cleaved caspase-3, normalized with actin, on DIV 14 and 15 in control cultures, cultures treated with repeated doses of 0.1/0.33/1 mM 2-MCA, or cultures treated with a single dose of 1 mM 2-MCA. At all 2-MCA concentrations, the highest levels of cleaved caspase-3 were observed on DIV 14. On DIV 15, cleaved caspase-3 expression returned to control levels, except for aggregates exposed to repeated doses of 1 mM 2-MCA. (C) Western blot for cleaved caspase-3 and calpain cleaved α-fodrin, normalized with total α-fodrin, on DIV 14 and 15 in control cultures, cultures treated with repeated doses of 0.1/0.33/1 mM 2-MCA or cultures treated with a single dose of 1 mM 2-MCA. Data shown as mean ± SD ($n = 3$), Student's t-test: $^{*}p < 0.05$, $^{**}p < 0.01$, $^{***}p < 0.001$.

the first administration. The observation that NH_4^+ production increased rapidly after exposure to 2-MCA suggests that this may be the first pathogenic event, triggering further cellular and metabolic responses. NH_4^+ accumulation can result from excessive production or reduced detoxification mechanisms. As the 3D rat brain cell aggregate model contains exclusively brain cells and is a closed system, an alteration of the brain cell metabolism must be responsible for the accumulation of NH_4^+.

Major pathways for cerebral NH_4^+ production are (i) glutaminase activity, which converts glutamine to glutamate, (ii) glutamate dehydrogenase (GDH), which catalyzes oxidative deamination of glutamate in the astrocytes to release NH_4^+ for glutamine synthesis [31], and (iii) the purine nucleotide cycle, which converts L-aspartate to fumarate [32]. As organ, the brain is unable to detoxify NH_4^+ by producing urea because it does not express the full enzyme set of urea cycle. Hence, other reactions are responsible for NH_4^+ detoxification in the brain. The predominant one is the GS reaction, which converts brain NH_4^+ to glutamine. The second pathway for cerebral NH_4^+ detoxification is the reductive amination of α-ketoglutarate by GDH, which catalyzes glutamate synthesis in the neuron in order to capture the NH_4^+ released by phosphate-activated glutaminase [31]. The GS reaction leads to increased concentration of glutamine, whereas the GDH reaction results in increased concentration of alanine [32]. However, no change in glutamate or alanine levels was observed in our model.

In this study, GS activity was reduced in aggregates exposed to 2-MCA. As GS is mainly located in astrocytes [33], the reduced GS activity could result from astrocytic suffering and/or astrocyte loss by apoptotic cell death. Another possible explanation could be the induction of iNOS (inducible nitric oxide synthase) expression by excessive NH_4^+ concentration, since an increase in cerebral nitric oxide stimulates peroxynitrite-mediated nitration of tyrosine residues of GS, resulting in inactivation of GS [34]. Thereby, production of NO induced by NH_4^+ can inhibit GS and aggravate NH_4^+ accumulation [35,36].

We also observed that glutamine levels decreased in culture medium and increased intracellularly after exposure of aggregates to 2-MCA. Glutamine is considered as a mediator of NH_4^+ toxicity. According to the so-called "Trojan Horse" hypothesis, glutamine can be

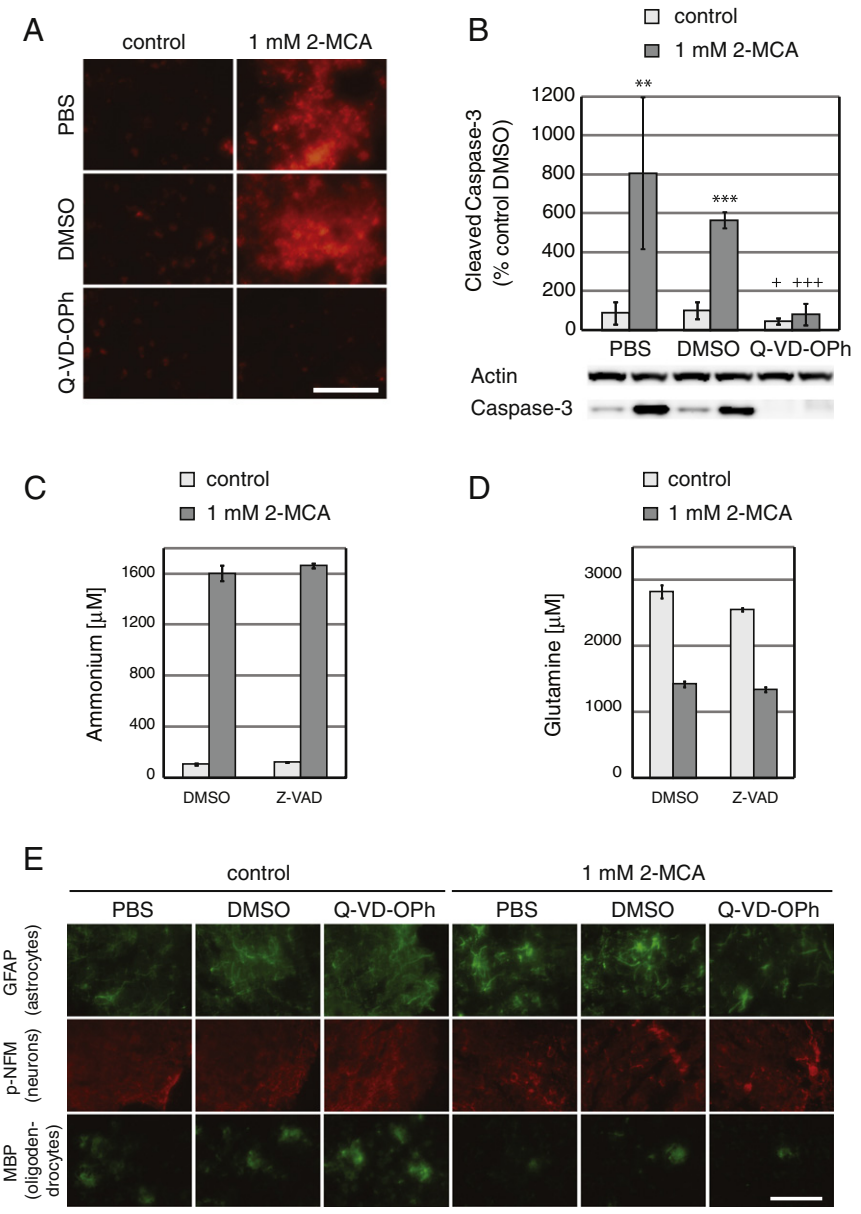

Fig. 9. Inhibition of apoptosis does not prevent 2-MCA-induced alterations in developing brain cells. (A) Immunofluorescence for cleaved caspase-3 on DIV 14 in control cultures and cultures treated with repeated doses of 1 mM 2-MCA, with additional administration of the pan-caspase inhibitor Q-VD-OPh. (B) Western blot for cleaved caspase-3, normalized with actin, on DIV 14 in control cultures and cultures treated with repeated doses of 1 mM 2-MCA, with additional administration of Q-VD-OPh. Data shown as mean ± SD ($n = 4$), control *vs* 2-MCA: Student's *t*-test: $^{*}p < 0.05$, $^{**}p < 0.01$, $^{***}p < 0.001$, control Q-VD-OPh *vs* control DMSO, 2-MCA Q-VD-OPh *vs* 2-MCA DMSO: Student's *t*-test: $+p < 0.05$, $+++p < 0.001$. Administration of Q-VD-OPh successfully inhibited cleaved caspase-3 activation under 2-MCA exposure. Concentration of DMSO (0.05%) used to solubilize Q-VD-OPH did not affect apoptosis rate. (C–D) NH_4^+ and glutamine levels were measured on DIV 14 in controls and cultures treated with repeated doses of 1 mM 2-MCA, with additional administration of pan-caspase inhibitor Z-VAD FMK. 2-MCA-induced NH_4^+ accumulation and glutamine decrease were not altered by treatment with Z-VAD FMK. Data shown as mean ± SD ($n = 2$). (E) Immunofluorescence for GFAP, p-NFM and MBP on DIV 14 in controls versus 1 mM 2-MCA-treated aggregates, with additional administration of Q-VD-OPh. Morphological alterations of astrocytes, neurons and oligodendrocytes observed under 2-MCA exposure occurred despite additional administration of Q-VD-OPh. Scale bar: 100 µm.

metabolized in mitochondria by phosphate-activated glutaminase, yielding glutamate and NH_4^+. In this manner, glutamine serves as an NH_4^+ carrier [37,38]. Thus, decreased glutamine in culture medium could also be due to the glutamine sink into mitochondria, in which glutamine would be converted to glutamate and NH_4^+. The fact that we did not observe any glutamate increase intracellularly does not contradict this hypothesis as excess glutamate in mitochondria can rapidly be converted to α-ketoglutarate in order to feed the TCA cycle, thus producing ammonium. However, seen the significant intracellular glutamine increase other mechanisms might be involved in its production.

Increased NH_4^+ levels are known to be toxic for the CNS. Moreover, the consequences of NH_4^+ toxicity are more devastating for a developing than for an adult brain [39,40]. Indeed, NH_4^+ is known to play a role in astrocyte swelling, alterations of glutamatergic neurotransmission, cerebral energy deficit, alteration of nitric oxide synthesis, impairment of axonal and dendritic growth, and cell death [40]. All these deleterious effects have been evoked to explain the neuropathogenesis of MMAuria [8,9,24].

4.2. 2-MCA induces astrocyte swelling, impairment of axonal growth and delayed myelination

Astrocyte swelling is the most pronounced morphological change observed under 2-MCA exposure, and it was already visible 17 h after the first exposure. Astrocytes are known to be prone to swelling in many clinical conditions, including hyperammonemia and hepatic

encephalopathy, ischemia and trauma [33,41]. The mechanisms leading to astrocytic swelling remain elusive. It is proposed that NH_4^+-induced oxidative stress initiates a cascade of events resulting in induction of the mitochondrial permeability transition and activation of intracellular signaling kinases. These events finally lead to the inability of astrocytes to regulate their intracellular volume, thus resulting in cell swelling [42]. Moreover, increased glutamine content in astrocytes is thought to be responsible for astrocyte swelling [40]. The decreased extracellular glutamine and the intracellular increase of glutamine content seen in our model could be responsible for astrocyte swelling.

Staining of aggregates treated with 2-MCA with the antibody against p-NFM suggest an impairment of axonal growth. This is in line with neuroimaging findings in MMAuria patients, who often manifest ventricular enlargement, cortical atrophy, periventricular white matter abnormalities, and thinning of the corpus callosum [43]. A previous study in 3D rat brain cells aggregates showed that NH_4^+ exposure leads to decreased NFM expression and phosphorylation and inhibition of axonal growth [44]. Moreover, astrocytes release several trophic factors which can stimulate neurite outgrowth [45]. If astrocytes are suffering, they might not be able to sustain axonal growth.

Interestingly, the morphological differences observed in astrocytes and neurons were less significant at the end of the experiment (DIV 19). This can be due to two different mechanisms: either the suffering cells undergo cell death and disappear; or, they are able to recover. Semi-quantitative determination of expression levels did not indicate any significant cell loss over time, thus making the hypothesis of recovery more likely.

The decreased MBP signal in aggregates treated with 2-MCA suggests a myelination delay, which is a common finding on brain imaging of MMAuria patients [43]. Axonal myelination is influenced by astrocytes. It is known that astrocytes secrete factors that directly affect oligodendrocytes [25,46]. Experimental models of demyelination demonstrated an important role for astrocytes in the subsequent remyelination [25]. It was shown that oligodendrocytes cannot myelinate demyelinated axons in areas devoid of astrocytes [47].

In conclusion, NH_4^+ accumulation in culture medium of 2-MCA treated aggregates is a very early event, and might be the cause of swelling of astrocytes. Impairment of axonal outgrowth and delayed myelination might be secondary effects determined by dysfunction of astrocytes.

4.3. 2-MCA increases the apoptotic rate

2-MCA exposure significantly increased cleaved caspase-3 levels in our model. Cleaved caspase-3 is mainly known to be a key protein in apoptosis execution. It has been shown in 3D brain cell cultures that NH_4^+ induced cell death by apoptosis [48]. Our data suggest that increased NH_4^+ concentrations might cause apoptosis in aggregates exposed to 2-MCA.

4.4. A single dose of 2-MCA is sufficient to induce deleterious damage

The second aim of this study was to compare the toxicity of a single dose of 1 mM 2-MCA with that observed with multiple doses.

Due to its low prevalence, MMAuria is often misrecognized. This leads to delay in diagnosis and introduction of appropriate treatment. Therefore, irreversible brain damage might already be present at diagnosis. In some countries, MMAuria is part of the newborn screening program. Thus, affected patients could be treated pre-symptomatically and avoid severe sequels. However, some patients still manifest neurologic impairment in spite of early diagnosis [49].

The “repeated treatment” protocol applied in this study mimics a situation with increasing amounts of circulating metabolites during several days. This situation might represent an undiagnosed MMAuria patient with delayed diagnosis and treatment after the onset of symptoms. Meanwhile, the toxic metabolites continue to accumulate until the appropriate treatment is introduced. On the other hand, the “single dose” treatment protocol reflects the situation of a well-known patient undergoing a febrile infection with prompt initiation of emergency treatment. Both situations were compared to evaluate their impact on brain injuries.

A single dose of 1 mM 2-MCA was found to be sufficient to induce deleterious effects in 3D rat brain cell aggregates. This result is in line with the clinical observation that brain damage can occur in known MMAuria patients suffering a metabolic decompensation despite early introduction of adequate treatment.

5. Conclusions and perspectives

This study shows that ammonium accumulation is an early and primary effect of 2-MCA exposure in our *in vitro* model for brain damage in MMAuria. As a second significant result, we now can exclude that ammonium accumulation is the consequence of significant cell death by apoptosis, as ammonium increased in the same manner after inhibition of apoptosis. Finally, a single dose of 1 mM 2-MCA was as efficient in inducing ammonium accumulation and cytopathologic changes as a prolonged exposure. If translated to the *in vivo* situation of patients affected by MMAuria or propionic aciduria, this might imply that during a catabolic state, an increase of 2-MCA in the brain might rapidly induce intracerebral NH_4^+ accumulation. This early event could be the trigger for other biochemical and morphological alterations, including cell death by apoptosis, suggesting a potential danger for brain damage in every metabolic decompensation, even for short duration, once a critical threshold of intracerebral 2-MCA concentrations has been passed. Further studies should focus on the elucidation of the biochemical pathways leading to NH_4^+ accumulation in our model and verify if this observation obtained can be confirmed *in vivo*. A deeper understanding of the implicated pathways might give us indications for the development of neuroprotective strategies in MMAuria.

Acknowledgements

We thank Marc Loup for technical assistance, Dominique Werner for organization and supervision of routine metabolite measurements and Julien Puyal for critical discussion. We are very grateful for the input of Andrea Superti-Furga on the redaction of this manuscript. This work was supported by the Swiss National Science Foundation [grant number 310030-153071]; and the Novartis Foundation for Medical-Biological Research [grant number 13C171].

References

[1] F. Deodato, S. Boenzi, F.M. Santorelli, C. Dionisi-Vici, Methylmalonic and propionic aciduria, Am. J. Med. Genet. C: Semin. Med. Genet. 142C (2) (2006) 104–112.
[2] B. Fowler, J.V. Leonard, M.R. Baumgartner, Causes of and diagnostic approach to methylmalonic acidurias, J. Inherit. Metab. Dis. 31 (3) (2008) 350–360.
[3] L. Van Gosen, Organic acidemias: a methylmalonic and propionic focus, J. Pediatr. Nurs. 23 (3) (2008) 225–233.
[4] M.R. Seashore, The organic acidemias: an overview, in: R.A. Pagon, M.P. Adam, H.H. Ardinger, S.E. Wallace, A. Amemiya, L.J.H. Bean, et al., (Eds.), Gene Reviews®, University of Washington, Seattle, WA, 1993-2016.
[5] M.A. Cosson, J.F. Benoist, G. Touati, M. Déchaux, N. Royer, L. Grandin, et al., Long-term outcome in methylmalonic aciduria: a series of 30 French patients, Mol. Genet. Metab. 97 (3) (2009) 172–178.
[6] M. Nizon, C. Ottolenghi, V. Valayannopoulos, J.B. Arnoux, V. Barbier, F. Habarou, et al., Long-term neurological outcome of a cohort of 80 patients with classical organic acidurias, Orphanet J. Rare Dis. 8 (2013) 148.
[7] F. Hörster, M.R. Baumgartner, C. Viardot, T. Suormala, P. Burgard, B. Fowler, et al., Long-term outcome in methylmalonic acidurias is influenced by the underlying defect (mut0, mut-, cblA, cblB), Pediatr. Res. 62 (2) (2007) 225–230.
[8] M.A. Morath, J.G. Okun, I.B. Muller, S.W. Sauer, F. Hörster, G.F. Hoffmann, et al., Neurodegeneration and chronic renal failure in methylmalonic aciduria–a pathophysiological approach, J. Inherit. Metab. Dis. 31 (1) (2008) 35–43.
[9] D.R. Melo, A.J. Kowaltowski, M. Wajner, R.F. Castilho, Mitochondrial energy metabolism in neurodegeneration associated with methylmalonic acidemia, J. Bioenerg. Biomembr. 43 (1) (2011) 39–46.
[10] S. Kölker, S.W. Sauer, R.A. Surtees, J.V. Leonard, The aetiology of neurological complications of organic acidaemias–a role for the blood-brain barrier, J. Inherit. Metab. Dis. 29 (6) (2006) 701–704 discussion 5–6.

[11] D. Ballhausen, L. Mittaz, O. Boulat, L. Bonafé, O. Braissant, Evidence for catabolic pathway of propionate metabolism in CNS: expression pattern of methylmalonyl-CoA mutase and propionyl-CoA carboxylase alpha-subunit in developing and adult rat brain, Neuroscience 164 (2) (2009) 578–587.
[12] S. Kölker, J.G. Okun, Methylmalonic acid–an endogenous toxin? Cell. Mol. Life Sci.: CMLS 62 (6) (2005) 621–624.
[13] C.G. Fernandes, C.G. Borges, B. Seminotti, A.U. Amaral, L.A. Knebel, P. Eichler, et al., Experimental evidence that methylmalonic acid provokes oxidative damage and compromises antioxidant defenses in nerve terminal and striatum of young rats, Cell. Mol. Neurobiol. 31 (5) (2011) 775–785.
[14] S. Kölker, M. Schwab, F. Hörster, S. Sauer, A. Hinz, N.I. Wolf, et al., Methylmalonic acid, a biochemical hallmark of methylmalonic acidurias but no inhibitor of mitochondrial respiratory chain, J. Biol. Chem. 278 (48) (2003) 47388–47393.
[15] D.R. Melo, S.R. Mirandola, N.A. Assunção, R.F. Castilho, Methylmalonate impairs mitochondrial respiration supported by NADH-linked substrates: involvement of mitochondrial glutamate metabolism, J. Neurosci. Res. 90 (6) (2012) 1190–1199.
[16] J.G. Okun, F. Hörster, L.M. Farkas, P. Feyh, A. Hinz, S. Sauer, et al., Neurodegeneration in methylmalonic aciduria involves inhibition of complex II and the tricarboxylic acid cycle, and synergistically acting excitotoxicity, J. Biol. Chem. 277 (17) (2002) 14674–14680.
[17] M. Wajner, J.C. Coelho, Neurological dysfunction in methylmalonic acidaemia is probably related to the inhibitory effect of methylmalonate on brain energy production, J. Inherit. Metab. Dis. 20 (6) (1997) 761–768.
[18] S. Cheema-Dhadli, C.C. Leznoff, M.L. Halperin, Effect of 2-methylcitrate on citrate metabolism: implications for the management of patients with propionic acidemia and methylmalonic aciduria, Pediatr. Res. 9 (12) (1975) 905–908.
[19] A.R. Horswill, A.R. Dudding, J.C. Escalante-Semerena, Studies of propionate toxicity in Salmonella enterica identify 2-methylcitrate as a potent inhibitor of cell growth, J. Biol. Chem. 276 (22) (2001) 19094–19101.
[20] C.J. Rocco, J.C. Escalante-Semerena, In Salmonella enterica, 2-methylcitrate blocks gluconeogenesis, J. Bacteriol. 192 (3) (2010) 771–778.
[21] P. Honegger, Aggregating neural cell cultures, in: M.D. Maines (Ed.), Current Protocols in Toxicology, 2003 editorial board. Chapter 12:Unit 12.9.
[22] P. Honegger, A. Defaux, F. Monnet-Tschudi, M.G. Zurich, Preparation, maintenance, and use of serum-free aggregating brain cell cultures, Methods Mol. Biol. 758 (2011) 81–97.
[23] M.G. Zurich, S. Stanzel, A. Kopp-Schneider, P. Prieto, P. Honegger, Evaluation of aggregating brain cell cultures for the detection of acute organ-specific toxicity, Toxicol. In Vitro 27 (4) (2013) 1416–1424.
[24] P. Jafari, O. Braissant, P. Zavadakova, H. Henry, L. Bonafé, D. Ballhausen, Brain damage in methylmalonic aciduria: 2-methylcitrate induces cerebral ammonium accumulation and apoptosis in 3D organotypic brain cell cultures, Orphanet J. Rare Dis. 8 (2013) 4.
[25] L. Cagnon, O. Braissant, CNTF protects oligodendrocytes from ammonia toxicity: intracellular signaling pathways involved, Neurobiol. Dis. 33 (1) (2009) 133–142.
[26] O. Braissant, L. Cagnon, F. Monnet-Tschudi, O. Speer, T. Wallimann, P. Honegger, et al., Ammonium alters creatine transport and synthesis in a 3D culture of developing brain cells, resulting in secondary cerebral creatine deficiency, Eur. J. Neurosci. 27 (7) (2008) 1673–1685.
[27] O.H. Lowry, N.J. Rosebrough, A.L. Farr, R.J. Randall, Protein measurement with the Folin phenol reagent, J. Biol. Chem. 193 (1) (1951) 265–275.
[28] A.J. Patel, A. Hunt, R.D. Gordon, R. Balázs, The activities in different neural cell types of certain enzymes associated with the metabolic compartmentation glutamate, Dev. Brain Res. 4 (1982) 3–11.
[29] M.R. Pishak, A.T. Phillips, A modified radioisotopic assay for measuring glutamine synthetase activity in tissue extracts, Anal. Biochem. 94 (1979) 82–88.
[30] P. Honegger, O. Braissant, H. Henry, O. Boulat, C. Bachmann, M.G. Zurich, et al., Alteration of amino acid metabolism in neuronal aggregate cultures exposed to hypoglycaemic conditions, J. Neurochem. 81 (6) (2002) 1141–1151.
[31] D.L. Rothman, H.M. De Feyter, P.K. Maciejewski, K.L. Behar, Is there in vivo evidence for amino acid shuttles carrying ammonia from neurons to astrocytes? Neurochem. Res. 37 (11) (2012) 2597–2612.
[32] A.J. Cooper, The role of glutamine synthetase and glutamate dehydrogenase in cerebral ammonia homeostasis, Neurochem. Res. 37 (11) (2012) 2439–2455.
[33] M.D. Norenberg, A. Martinez-Hernandez, Fine structural localization of glutamine synthetase in astrocytes of rat brain, Brain Res. 161 (2) (1979) 303–310.
[34] B. Görg, M. Wettstein, S. Metzger, F. Schliess, D. Häussinger, Lipopolysaccharide-induced tyrosine nitration and inactivation of hepatic glutamine synthetase in the rat, Hepatology 41 (5) (2005) 1065–1073.
[35] V. Felipo, R.F. Butterworth, Neurobiology of ammonia, Prog. Neurobiol. 67 (4) (2002) 259–279.
[36] C.F. Rose, A. Verkhratsky, V. Parpura, Astrocyte glutamine synthetase: pivotal in health and disease, Biochem. Soc. Trans. 41 (6) (2013) 1518–1524.
[37] J. Albrecht, M.D. Norenberg, Glutamine: a Trojan horse in ammonia neurotoxicity, Hepatology 44 (4) (2006) 788–794.
[38] K.V. Rama Rao, M.D. Norenberg, Glutamine in the pathogenesis of hepatic encephalopathy: the trojan horse hypothesis revisited, Neurochem. Res. 39 (3) (2014) 593–598.
[39] C. Bachmann, Mechanisms of hyperammonemia, Clin. Chem. Lab. Med.: CCLM/FESCC 40 (7) (2002) 653–662.
[40] O. Braissant, V.A. McLin, C. Cudalbu, Ammonia toxicity to the brain, J. Inherit. Metab. Dis. 36 (4) (2013) 595–612.
[41] M. Sidoryk-Wegrzynowicz, M. Wegrzynowicz, E. Lee, A.B. Bowman, M. Aschner, Role of astrocytes in brain function and disease, Toxicol. Pathol. 39 (1) (2011) 115–123.
[42] M.D. Norenberg, A.R. Jayakumar, K.V. Rama Rao, K.S. Panickar, New concepts in the mechanism of ammonia-induced astrocyte swelling, Metab. Brain Dis. 22 (3–4) (2007) 219–234.
[43] E.H. Baker, J.L. Sloan, N.S. Hauser, A.L. Gropman, D.R. Adams, C. Toro, et al., MRI characteristics of globus pallidus infarcts in isolated methylmalonic acidemia, AJNR Am. J. Neuroradiol. 36 (1) (2015) 194–201.
[44] O. Braissant, H. Henry, A.M. Villard, M.G. Zurich, M. Loup, B. Eilers, et al., Ammonium-induced impairment of axonal growth is prevented through glial creatine, J. Neurosci. 22 (22) (2002) 9810–9820.
[45] J.L. Ridet, S.K. Malhotra, A. Privat, F.H. Gage, Reactive astrocytes: cellular and molecular cues to biological function, Trends Neurosci. 20 (12) (1997) 570–577.
[46] S.C. Barnett, C. Linington, Myelination: do astrocytes play a role? Neuroscientist 19 (5) (2013) 442–450.
[47] W.H. Norton, M. Mangoli, Z. Lele, H.M. Pogoda, B. Diamond, S. Mercurio, et al., Monorail/Foxa2 regulates floorplate differentiation and specification of oligodendrocytes, serotonergic raphe neurones and cranial motoneurones, Development 132 (4) (2005) 645–658.
[48] L. Cagnon, O. Braissant, Role of caspases, calpain and cdk5 in ammonia-induced cell death in developing brain cells, Neurobiol. Dis. 32 (2) (2008) 281–292.
[49] C. Dionisi-Vici, F. Deodato, W. Röschinger, W. Rhead, B. Wilcken, 'Classical' organic acidurias, propionic aciduria, methylmalonic aciduria and isovaleric aciduria: long-term outcome and effects of expanded newborn screening using tandem mass spectrometry, J. Inherit. Metab. Dis. 29 (2–3) (2006) 383–389.